Energy 200 (2020) 117555

Contents lists available at ScienceDirect

Energy

journal homepage: www.elsevier.com/locate/energy

Robust optimization strategy for intelligent parking lot of electric vehicles

Jianwei Guo [a, **], Yongbo Lv [a], Han Zhang [a], Sayyad Nojavan [b], Kittisak Jermsittiparsert [c, *]

[a] School of Traffic and Transportation, Beijing Jiaotong University, Beijing, 100044, China
[b] Department of Electrical Engineering, University of Bonab, Bonab, Iran
[c] Social Research Institute, Chulalongkorn University, Bangkok, 10330, Thailand

ARTICLE INFO

Article history:
Received 6 February 2020
Received in revised form
2 April 2020
Accepted 4 April 2020
Available online 9 April 2020

Keywords:
Electric vehicles (EVs)
Intelligent parking lot (IPL)
Bidding curve
Power price uncertainty
Optimal energy management
Robust optimization approach

ABSTRACT

In this paper the concept of intelligent parking lot (IPL) is proposed to csolve various challenges of electric vehicles (EVs) integration into the power system. Robust optimization approach is proposed to model the power price uncertainty and obtain the optimal bidding curves of IPL for each hour in order to submit to the power market. Using the provided optimal bidding curves, system operator can get required power to satisfy demand of the system with economical price under power price uncertainty. Optimal scheduling of each component of the system is studied in three different strategies as optimistic, deterministic, and pessimistic to consider all possible cases raised by the power price uncertainty. Each strategy has been solved in two cases as with and without demand response program (DRP). The applied DRP has reduced system operating cost through flattening the load curve. By comparing ROA results with the deterministic case, the total operating cost of the system is decreased from $1029 to $995 about 17.85% decrease while in pessimistic strategy, it is increased from $1209 to $1333 indicating about 9.85% increase. The problem has been solved using GAMS optimization software with the CPLEX solver.

1. Introduction

By increasing related concerns to greenhouse gas emissions, scientists try to find and develop new ways to reduce greenhouse gas emissions [1]. As it can be seen from Fig. 1, considerable part of the emission is generated by the transportation systems in Ontario [2]. To reduce the transportation systems portion, replacing common combustion-based engine vehicles by electric vehicles (EVs) can be a reliable and feasible idea [3]. By advance in technology, performance of EVs gets better day by day which draw attentions toward using them instead of common transportation vehicles [4]. By the estimations of the electric power system research institute (EPRI), about 62% of transportation system will be replaced by EVs at the end of 2050 [5]. Integration of high number of EVs into the current power system can impose new challenges on operation of power systems, especially at the distribution level [6]. The subject goes worse when considering high uncertainty of EVs. EVs are dispersed all over the distribution network and power consumption of EVs is a function of drivers' behavior which varies from a person to another. Therefore, integration of EVs into the power system should be studies exactly.

The concept of intelligent parking lots (IPLs) of EVs can be taken into account as one of the most reliable and feasible solutions to integrate EVs in the power systems [7]. The IPLs can be taken into account as a charging point for numerous EVs. In this way, by optimal planning of the IPLs, not only their negative effects can be removed, but also they can be considered as an energy source which can be used to flatten load curve, a source of ancillary services in the system, etc. Therefore, in this paper, optimal contribution of IPLs in the power market is studied by developing a novel robust strategy to provide optimal bidding curves. The procedure is detailed in the next sections.

1.1. Literature review

As said before, the IPL concept has been drawn many attentions to integrate the EVs in the power systems which will be discussed as follows. In Ref. [8], interconnection of upstream-grid and EVs is studied by proposing novel ideas of parking-to-vehicle, and

* Corresponding author.
** Corresponding author.
E-mail addresses: 19114023@bjtu.edu.cn (J. Guo), sayyad.nojvan@bonabu.ac.ir (S. Nojavan), kittisak.j@chula.ac.th (K. Jermsittiparsert).

https://doi.org/10.1016/j.energy.2020.117555
0360-5442/

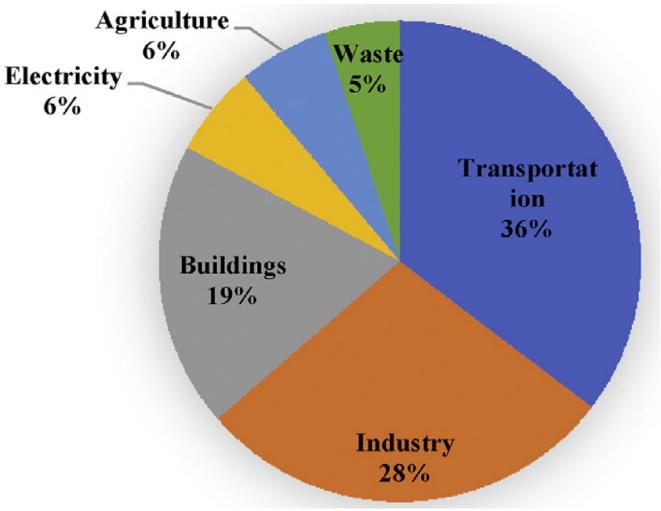

Fig. 1. Emission of greenhouse gases in Ontario in 2013 [2].

vehicle-to-parking instead of grid-to-vehicle, vehicle-to-grid concepts. By deploying the Game theory method, discharging/charging behaviors of EVs is investigated in Ref. [9]. By using two stages approximate dynamic programming framework, EVs optimal scheduling is considered by dividing different places into commercial and residential ones and considering their behaviors in night and day intervals in Ref. [10]. Discharge of EVs is studied in a personal parking lot based on driving patterns of EV owners in Ref. [11]. By taking owner of EVs requirements into account, the EVs discharge in reserve and joint energy markets are surveyed in Ref. [12]. By utilizing a probabilistic method, optimal placement for parking lot of EVs is investigated based on uncertain driving patterns of EV owners for a distribution network [13]. In Ref. [14], a fuzzy system is suggested to provide a real-time connection between EVs and the operator of the distribution system. A novel probabilistic method to accurately verify the voltage constraints requirements of radial distribution systems is developed in the presence of photovoltaic systems and EVs in Ref. [15]. To do so, first, the PV systems and EV charging loads are modeled as random variables. Also, in order to confirm the accuracy of the obtained results of proposed probabilistic method, a Monte Carlo simulation was carried out. To optimize the sizing and power management of EV charging load, a novel model is proposed in Ref. [16]. To calculate the revenue and costs, the proposed model utilizes an annual techno-economic assessment by methods of the teaching learning based optimization algorithm. A general analytical technique for assessment and modeling of the combined technical aspects of EVs and photovoltaic plant in radial distribution network is proposed in Ref. [17] considering a one-year time period. Capacity of IPL discharge is estimated by a novel mathematical model for a roof top PV equipped IPL in Ref. [18]. In order to participate in reserve market, a novel model is proposed considering battery capacities of EVs in the IPL in Ref. [19]. In Refs. [20], a parking lot is converted to an IPL with the aim of discharge/charge of EVs in high amount. To maximize the amount energy sale which is stored in the parked EVs in the IPL, various parameters are developed in Ref. [21]. In an urban IPL, optimal energy planning of high EV number is surveyed in Ref. [22]. Considering different uncertain parameter, a stochastic scheduling for charging and discharging of parked EVs in an IPL is utilized in Ref. [23]. To discharge and charge an EV in an optimal way, stochastic dynamic programming model is suggested in Ref. [24]. With the goal of minimizing operational cost and greenhouse gases emission, a bi-objective model which is solved using ε-constraint method is proposed in Ref. [25]. In Ref. [26–28], a multi-objective model is suggested to optimally determine the location and size of an IPL taking different issues such as distribution system reliability into account. In Ref. [29], to analyze EV's charging/discharging a deterministic model is proposed based on the chain Markov-chain model.

1.2. Novelty and contribution

As we discussed above, many worthy works have been reported on optimal operation and planning of IPL. Although, according to our knowledge, participation of IPLs in the power market considering various uncertain parameter such as power price has not been well-studied yet. Therefore, in this paper, providing optimal bidding curves which will be provided to the day-ahead power market is pursued using the robust optimization method. To get better realization of various uncertain parameters' impact on operation of the IPL, three different strategies as pessimistic, deterministic, and optimistic are developed in which the pessimistic strategy seeks out increase of power price in the upstream-grid while the optimistic strategy considers possible power price reduction in the system. Meanwhile, deterministic strategy presents optimal scheduling results of the IPL without considering power price uncertainty. To decrease the system operating cost, the DRP is considered as a powerful tool to manage load demand of the system in which two cases as with DRP and without DRP are considered to solve the problem in each strategy. Finally, it should be noted that the problem has been formulated as robust mixed-integer programming (RMIP) which is solved using the GAMS optimization software with the CPLEX solver. The contribution and novelty of this paper can be briefly considered as:

1. Proposing IPL concept to integrate huge number of EVs into the power systems
2. Providing optimal hourly bidding curves for IPL using ROA.
3. Proposing TOU of DRP as a virtual generation unit to decrease load and system operation cost.
4. Providing three different strategies as optimistic, deterministic, and pessimistic strategies to cover all possible operation condition of the system under power price uncertainty

1.3. Paper organization

The paper's reminder contains following sections: Section 2 provides the deterministic formulation of the problem. Section 3 gives detail of implementing of robust optimization approach (ROA) on the problem. Section 4 presents the obtained results in all strategies and Section 5 provides discussion to the paper. Finally, Section 6 concludes the paper.

2. Deterministic formulation

Fig. 2 presents the under study system which is composed of different parts as wind-turbine, micro turbines, IPL, fuel cell, hydrogen storage system, load, and DRP as virtual generation units. Each part of the system will be detailed in the following system. In addition, the system is considered in the grid-connected model which gives opportunity to interchange energy with the upstream-grid.

2.1. Objective function

The objective function of the system is designed to minimize total operating cost of the system which is shown by Eq. (1). The

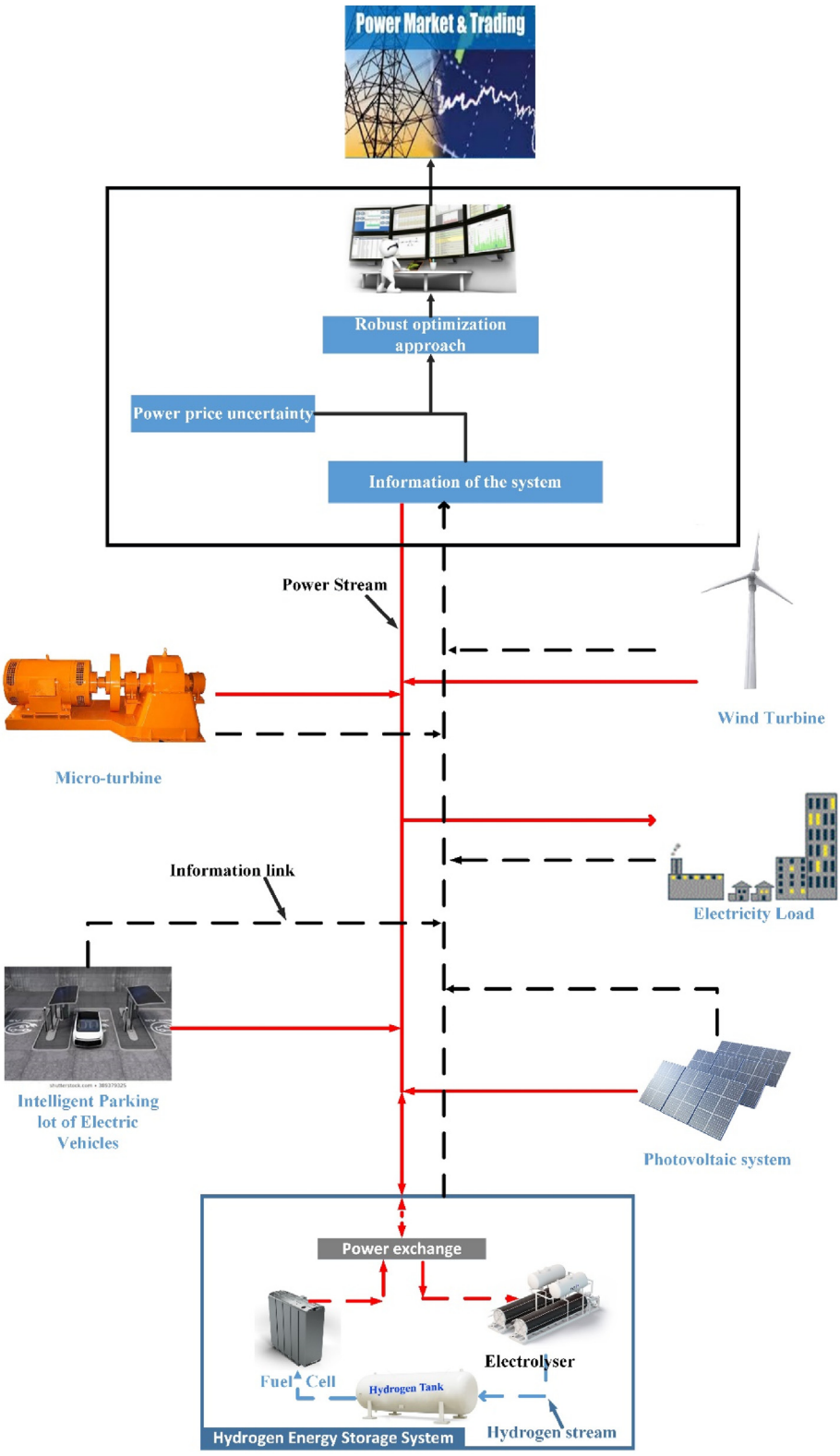

Fig. 2. Configuration of the under-study system.

objective function (1) is composed of three main part in which present power procurement cost from upstream grid, micro turbines (MTs), and energy exchange cost of the IPL, respectively. The second term, which refers to operating cost of the MTs, is consisted of two term to model operating and start-up costs such units. In the last term which is developed to model operating cost of the IPL, charging of EVs are considered as negative while discharging of EVs are assumed positive. This assumption comes from the charging EVs in the IPL will make profit for the operator of the IPL. Therefore, it should be considered as negative parameter as the objective

function is designed based on operating costs of the system.

$$OBJ = \sum_{t=1}^{T}\left[\left(P_{UG}^{t}\times\pi_{UG}^{t}+\sum_{j=1}^{G}\left(C_{LDG}^{j,t}+SC_{LDG}^{j,t}\right)+\sum_{i=1}^{N}\left(-P_{Ch,EV}^{i,t}\times\pi_{Ch,EV}^{i}+P_{Dch,EV}^{i,t}\times\pi_{Dch,EV}^{i}\right)\right)\times\Delta t\right] \tag{1}$$

where.

P_{UG}^{t} is the purchased power from the upstream-grid

π_{UG}^{t} is the power price in the upstream grid

$C_{LDG}^{j,t}$ is the operation cost of micro-turbine units.

$SC_{LDG}^{j,t}$ is the start-up cost of micro-turbine units

$P_{Ch,Ev}^{i,t}$ is the EVs' charged power.

$P_{Dch,Ev}^{i,t}$ is the EVs' discharged power.

$\pi_{Ch,Ev}^{i}$ is the price of charged power of electric vehicles in the IPL

$\pi_{Dch,Ev}^{i}$ is the price of discharged power of EVs in the IPL

Δt is the sampling time to count parked EVs in the IPL.

2.2. Power balance constraint

In order to make balance between load of system and supply in at any time, the load balance limitation is provided in constraint (2). In this constraint, the amount of load in the system is obtained after implementation of the DRP which will be detailed in the next subsection.

$$P_{UG}^{t}+\sum_{k=1}^{K}P_{W}^{k,t}+\sum_{p=1}^{P}P_{PV}^{p,t}+\sum_{j=1}^{G}P_{LDG}^{j,t}+\sum_{i=1}^{N}P_{Dch,EV}^{i,t}+P_{t}^{FC}=load^{t}+\sum_{i=1}^{N}P_{Ch,EV}^{i,t}+P_{t}^{EL} \tag{2}$$

where.

$P_{W}^{k,t}$ is power output of WT units

$P_{PV}^{p,t}$ is the power output of photovoltaic systems

$P_{LDG}^{j,t}$ is the scheduled generated power of micro-turbine units

P_{t}^{FC} is the injected power by the fuel-cell

$load^{t}$ is the load demand after implementing time of use rate of DRP

P_{t}^{EL} is the power consumption of the electrolyser to generate hydrogen molar.

2.3. Demand response program modeling

In order to make balance between load and supply, flatten the load curve, reducing the total operating cost, etc. different types of demand response programs are developed and frequently used in the power systems which are detailed in Refs. [30]. In this paper, the time-of-use (TOU) rate of DRP is considered to reduce total operating cost of the system which is provided in Eqs. (2)–(6). Proposed DRP shifts demand from expensive period to low price period without reducing total load amount of the system which provides many benefits such as loss reduction in peak periods, flattening the load and most importantly operating cost reduction in the system [31]. The load demand of the system after implementing DRP is provided by Eq. (3). In order to restrict shifted load from one period to another, Eqs. (4) and (5) are deployed. In this paper, DRP can only shift 20% of base-load from one period to another. Finally, Eq. (6) is used to make sure that the load is shifted from peak-price periods to off-peak-price periods [32].

$$load^{t}=load_{0}^{t}+DRP^{t} \tag{3}$$

$$DRP^{t}\leq+DRP^{\max}\times load_{0}^{t} \tag{4}$$

$$DRP^{t}\geq-DRP^{\max}\times load_{0}^{t} \tag{5}$$

$$\sum_{t=1}^{T}DRP^{t}=0 \tag{6}$$

where.

$load_{0}^{t}$ is the base load demand of the system at time t

$DRP^{\max}$ is the maximum participation amount of consumers in DRP in percent

DRP^{t} is a variable for possibility of DRP implementation, when load is increased it takes positive values; otherwise negative.

2.4. Renewable energy sources model

As discussed before, WT and PV are considered as renewable energy generation sources in the system which are modeled by Eqs. (7) and (8), respectively. It is obvious that power output of WT is related to the wind speed and temperature and solar radiation are most important factors that affect power output of PV system [33].

$$P_{W}^{k,t}=\begin{cases}0 & V^{t}<V_{c}^{k}\ or\ V^{t}\geq V_{F}^{k}\\ \dfrac{V^{t}-V_{c}^{k}}{V_{R}^{k}-V_{c}^{k}}\times P_{R}^{k} & V_{c}^{k}\leq V^{t}<V_{R}^{k}\\ P_{R}^{k} & V_{R}^{k}\leq V^{t}<V_{F}^{k}\end{cases} \tag{7}$$

where.

V^{t} is the estimated wind-speed.

V_{F}^{k}/ V_{c}^{k}/V_{R}^{k} is the cut-out/cut-in/rated speed of WT

P_{R}^{k} is the rated power of WT

$$P_{PV}^{p,t}=\eta^{p}\times s^{p}\times G^{t}\times(1-0.005\times(T_{a}-25)) \tag{8}$$

where.

η^{p} is the conversion factor of PV array

s^{p} is the PV area

G^{t} is the solar radiation on PV panels

T_{a} is the temperature around the PV.

2.5. Micro-turbines model

As one of the main power sources of the considered system, the MT is model using Eqs. (9)-(11) in which Eqs. (10) and (11) model operation and startup costs of the MTs, respectively [23].

$$C_{LDG}^{j,t}=a^{j}\times U^{j,t}+b^{j}\times P_{LDG}^{j,t} \tag{9}$$

$$SC_{LDG}^{j,t}\geq\left(U^{j,t}-U^{j,t-1}\right)\times UDC^{j} \tag{10}$$

$$SC_{LDG}^{j,t}\geq 0 \tag{11}$$

where.

a^j and b^j are operation cost coefficients of the micro-turbine units

$U^{j,t}$ is the binary variable which is equal to 1 when the micro-turbine is ON; otherwise 0

UDC^j is the startup cost of DG.

In addition, operating constraints of the micro-turbines are provided by constraints (12)–(19). By using Eqs. (12) and (13), power output of the MTs are limited in its minimum and maximum level, respectively. The MTs' rates of ramp up and down are modeled by Eqs. (14)-(15). In addition, related constraints to the minimum-up and down time of the MTs, Eqs. (16)-(17) are implemented, respectively. Finally, to linearized the minimum-up and minimum-down time constraints, Eqs. (18) and (19) are considered, respectively [23].

$$P_{LDG}^{j,t} \geq P_{LDG,\min}^{j} \times U^{j,t} \tag{12}$$

$$P_{LDG}^{j,t} \leq P_{LDG,\max}^{j} \times U^{j,t} \tag{13}$$

$$P_{LDG}^{j,t} - P_{LDG}^{j,t-1} \leq RU^{j} \times U^{j,t} \tag{14}$$

$$P_{LDG}^{j,t-1} - P_{LDG}^{j,t} \leq RD^{j} \times U^{j,t-1} \tag{15}$$

$$U^{j,t} - U^{j,t-1} \leq U^{j,t+Up_{j,f}} \tag{16}$$

$$U^{j,t-1} - U^{j,t} \leq 1 - U^{j,t+Dn_{j,f}} \tag{17}$$

$$\mathrm{Up}_{\mathrm{j,f}} = \begin{Bmatrix} f & f \leq \mathrm{MUT_j} \\ 0 & f > \mathrm{MUT_j} \end{Bmatrix} \tag{18}$$

$$\mathrm{Dn}_{\mathrm{j,f}} = \begin{Bmatrix} f & f \leq \mathrm{MDT_j} \\ 0 & f > \mathrm{MDT_j} \end{Bmatrix} \tag{19}$$

where.

$P_{LDG,\min}^{j}/P_{LDG,\max}^{j}$ is the minimum/maximum power limits of the micro turbines

RD^j and RU^j are the ramp-down and ramp-up rates of the micro turbines, respectively.

2.6. Hydrogen storage system modeling

In the considered system, fuel-cell (FC), electrolyser (EL) and hydrogen storage tanks (HTS) are constituted a hydrogen storage system (HSS) which is considered to store energy during low price periods [34]. During low price periods, EL uses electricity power to generate hydrogen molar to be stored in the HTS. During high price periods, stored hydrogen in the tank is turned to the electricity power. In order to model HSS, Eqs. (20)-(32) are deployed [35]. Eqs. (20) and (21) limit power consumption of the EL in a maximum and minimum interval. The maximum amount hydrogen generation of the EL is limited by Eq. (22). Also, Eq. (23) is used to model hydrogen generation of the EL [35].

$$P_t^{EL} \leq P_{\max}^{EL} \times U_t^{EL} \tag{20}$$

$$P_t^{EL} \geq P_{\min}^{EL} \times U_t^{EL} \tag{21}$$

$$N_{H2,t}^{EL} \leq N_{H2,\max}^{EL} \times U_t^{EL} \tag{22}$$

$$N_{H2,t}^{EL} = \frac{\eta^{EL} P_t^{EL}}{LHV_{H2}} \tag{23}$$

where.

$P_{\max}^{EL}/P_{\min}^{EL}$ is the maximum/minimum power consumption limit of the EL

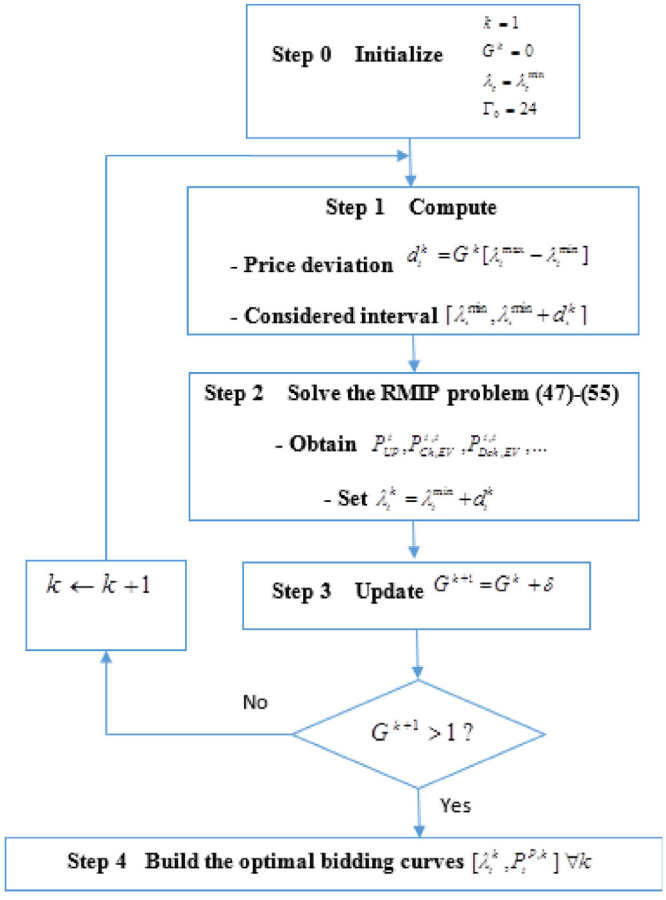

Fig. 3. Flowchart of proposed algorithm.

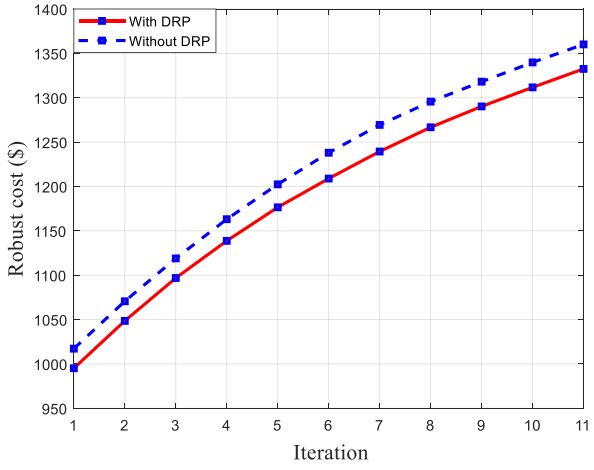

Fig. 4. Robust cost of the system.

Table 1
Summary of obtained results in different strategies.

	Optimistic strategy	Deterministic strategy	Pessimistic strategy
Without DRP ($)	1017	1238	1360
With DRP ($)	995.1	1209	1333
Change (%)	−2.15	−2.34	−1.98

U_t^{EL} is the binary-variable for operating status of EL
$N_{H2,t}^{EL}$ is the generated hydrogen molar by the EL
η^{EL} is the efficiency of EL
LHV_{H2} is the lower heating value of hydrogen.

Related constraints to the hydrogen tank including initial value, maximum, and minimum limits of the hydrogen tank are modeled by Eqs. (24)-(26), respectively [35].

$$P_{t0}^{H2} = P_{initial}^{H2} \tag{24}$$

$$P_t^{H2} \le P_{\max}^{H2} \tag{25}$$

$$P_t^{H2} \ge P_{\min}^{H2} \tag{26}$$

where.

P_{t0}^{H2} is the pressure of hydrogen tank at the beginning of the period.

$P_{initial}^{H2}$ is the hydrogen tank's initial pressure.
$P_{\max}^{H2}/P_{\min}^{H2}$ is the maximum/minimum hydrogen tank pressure
P_t^{H2} is the hydrogen tank pressure.

Maximum consumed hydrogen by the FC to generate electricity power is limited by Eq. (27). Eq. (28) is utilized to calculate the hydrogen consumption of FC, $N_{H2,t}^{FC}$ to generate electricity power P_t^{FC}. Also, Eqs. (27)-(30) are used to limit power generation of the FC [36].

$$N_{H2,t}^{FC} \le N_{H2,\max}^{FC} \times U_t^{FC} \tag{27}$$

$$N_{H2,t}^{FC} = \frac{P_t^{FC}}{\eta^{FC} LHV_{H2}} \tag{28}$$

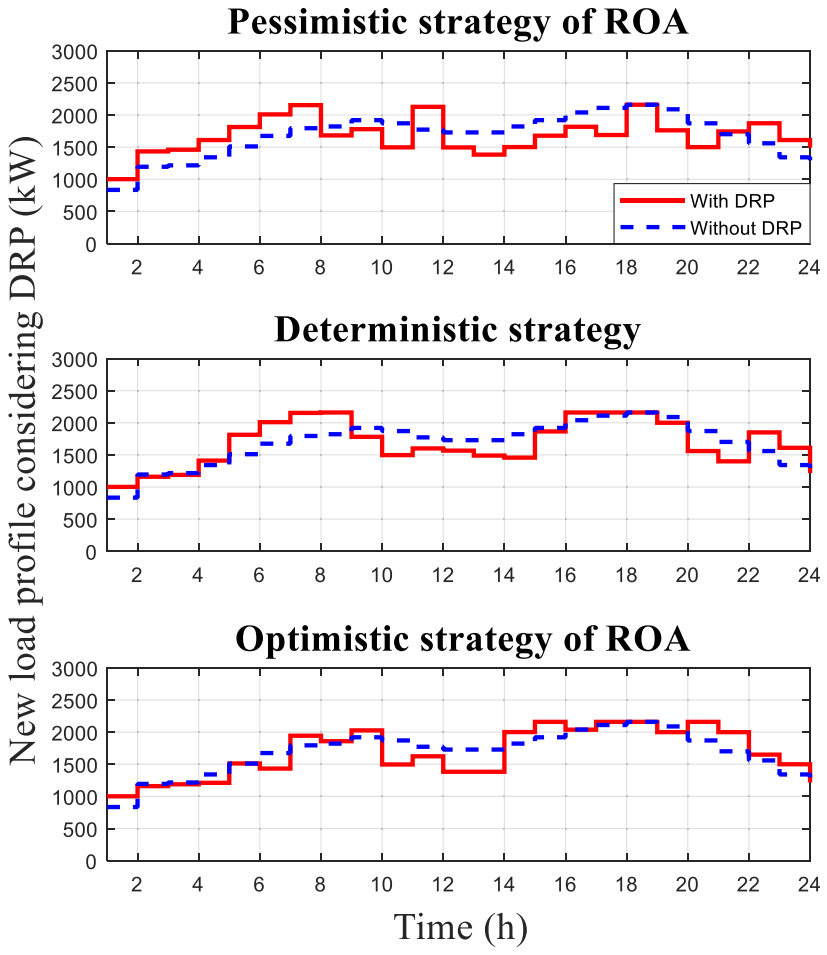

Fig. 5. Load profile of the system in all strategies.

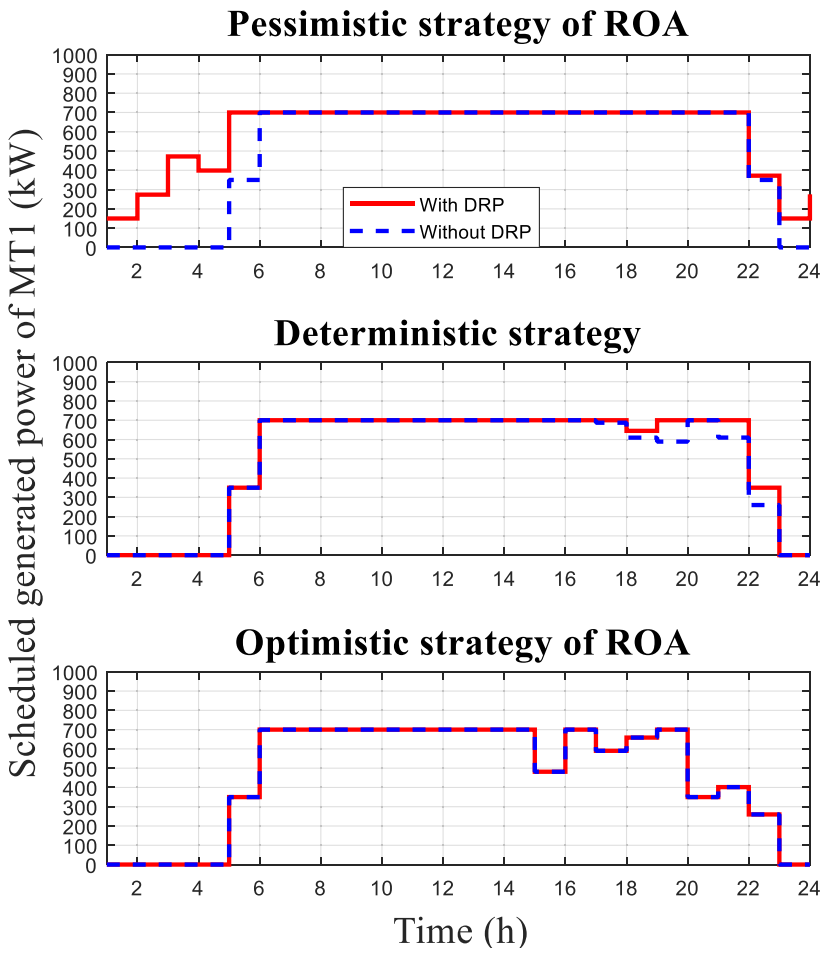

Fig. 6. Power generation of micro-turbine 1.

$$P_t^{FC} \le P_{\max}^{FC} \times U_t^{FC} \tag{29}$$

$$P_t^{FC} \ge P_{\min}^{FC} \times U_t^{FC} \tag{30}$$

where.

$N_{H2,t}^{FC}$ is the hydrogen molar consumption of the FC

$N_{H2,\max}^{FC}$ is the maximum hydrogen molar consumption limit of the FC

η^{FC} is the FC's efficiency.

$P_{\max}^{FC}/P_{\min}^{FC}$ is the FC's maximum/minimum output limit

P_t^{FC} is the produced power by FC

U_t^{FC} is the binary variable operation status of FC.

Simultaneous operation of EL and FC is prevented by applying Eq. (31). Finally, dynamic model of the HSS is modeled by Eq. (32) [35].

$$U_t^{EL} + U_t^{FC} \le 1 \tag{31}$$

$$P_t^{H2} = P_{t-1}^{H2} + \frac{\Re T_{H2}}{V_{H2}}\left(N_{H2,t}^{EL} - N_{H2,t}^{FC}\right) \tag{32}$$

where.

$\Re T_{H2}$is the gas constant

$V_{H2}$is the overall volume of the tank.

2.7. IPL model

As soon as the EVs enter to the IPL, IPL's operator gets various information from the EV owner to schedule the IPL. This information includes discharge/charge limits, elapsed battery life time, initial at arrival, expected SOC at departure etc. Then, to communicate the IPL and the upstream-grid, a central controller can be used to schedule the IPL optimally under operation condition of the upstream-grid. Operation of the IPL is modeled by constraints (33)–(41). Constraints (33)–(34) are applied to limit discharged and charged amount of power, respectively. To prevent charging and discharging of EVs at the same time, constraint (35) is considered. Maximum switching between discharge and charge states is constrained by Eq. (36). At each time t, SOC of the each EV is determined by Eq. (37). In order to restrict SOC of the EV between its maximum and minimum limits, constraint (38) is used [37].

$$P_{Dch,EV}^{i,t} \le P_{Dch,\max}^{i} \times W_{Dch}^{i,t} \times M^{i,t} \tag{33}$$

$$P_{Ch,EV}^{i,t} \le P_{Ch,\max}^{i} \times W_{ch}^{i,t} \times M^{i,t} \tag{34}$$

$$W_{ch}^{i,t} + W_{Dch}^{i,t} \le M^{i,t} \tag{35}$$

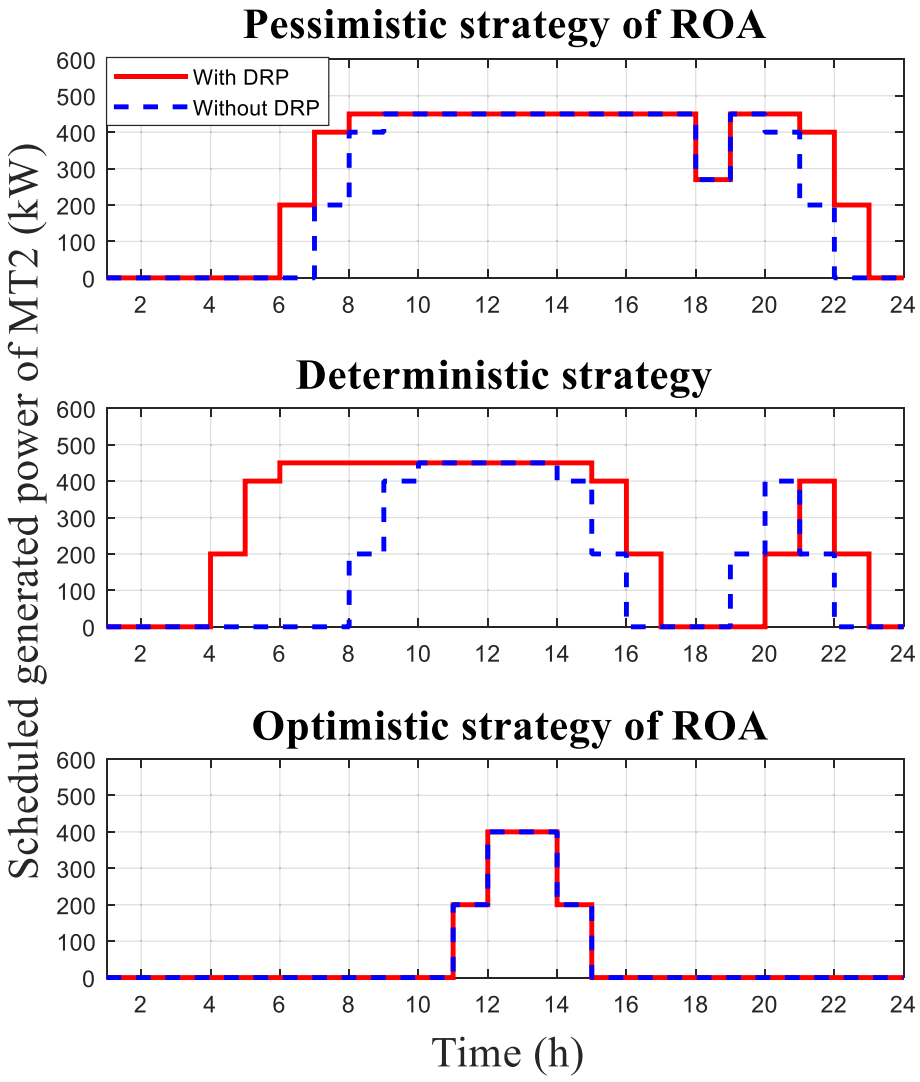

Fig. 7. Power generation of micro-turbine 2.

$$\sum_{t=t_a^i}^{t_d^i} W_{ch}^{i,t} + W_{Dch}^{i,t} \le N_{\max} \tag{36}$$

$$SOC^{i,t} = SOC^{i,t-1} + P_{Ch,EV}^{i,t} \times \eta_{G2V} - P_{Dch,EV}^{i,t} \Big/ \eta_{V2G} \tag{37}$$

$$SOC_{\min}^{i} \le SOC^{i,t} \le SOC_{\max}^{i} \tag{38}$$

where.

$P_{Ch,\max}^{i}$is the maximum charged power limit of the EV

$P_{Dch,\max}^{i}$is the maximum discharged power limit of the EV.

$W_{ch}^{i,t}/W_{Dch}^{i,t}$is the binary variable to determine charging and discharging modes of EV by assigning 1 and 0, respectively

$M^{i,t}$is a binary parameter to determine whether the EV is parked in IPL or not.

$SOC_{\max}^{i}/SOC_{\min}^{i}$ is the maximum/minimum SOC of EV

$SOC^{i,t}$is the SOC of EV at time t.

Considering different charging time of EVs, constraint (39) models maximum charge/discharge rates. To satisfy EV owners requested charge level at departure, constraint (40) is applied. Lastly, constraint (41) is utilized to make sure that EVs' SOC at each time is greater or equal to the their initial SOC [22].

$$-\Delta SOC_{\max}^{i} \le SOC^{i,t} - SOC^{i,t-1} \le \Delta SOC_{\max}^{i} \tag{39}$$

$$SOC_{\text{Departure}}^{\text{i,t}} \ge SOC_{\max}^{i} \tag{40}$$

$$SOC^{i,t} \ge SOC_{Arrival}^{i,t} \tag{41}$$

where.

$SOC_{Arrival}^{i,t}$is the EV's initial SOC

$SOC_{Departure}^{i,t}$is the SOC of EV in departure-time.

2.8. Constraint of power exchange with the upstream-grid

Finally, by using constraint (42), the energy interchange between upstream-grid and the IPL is restricted [30].

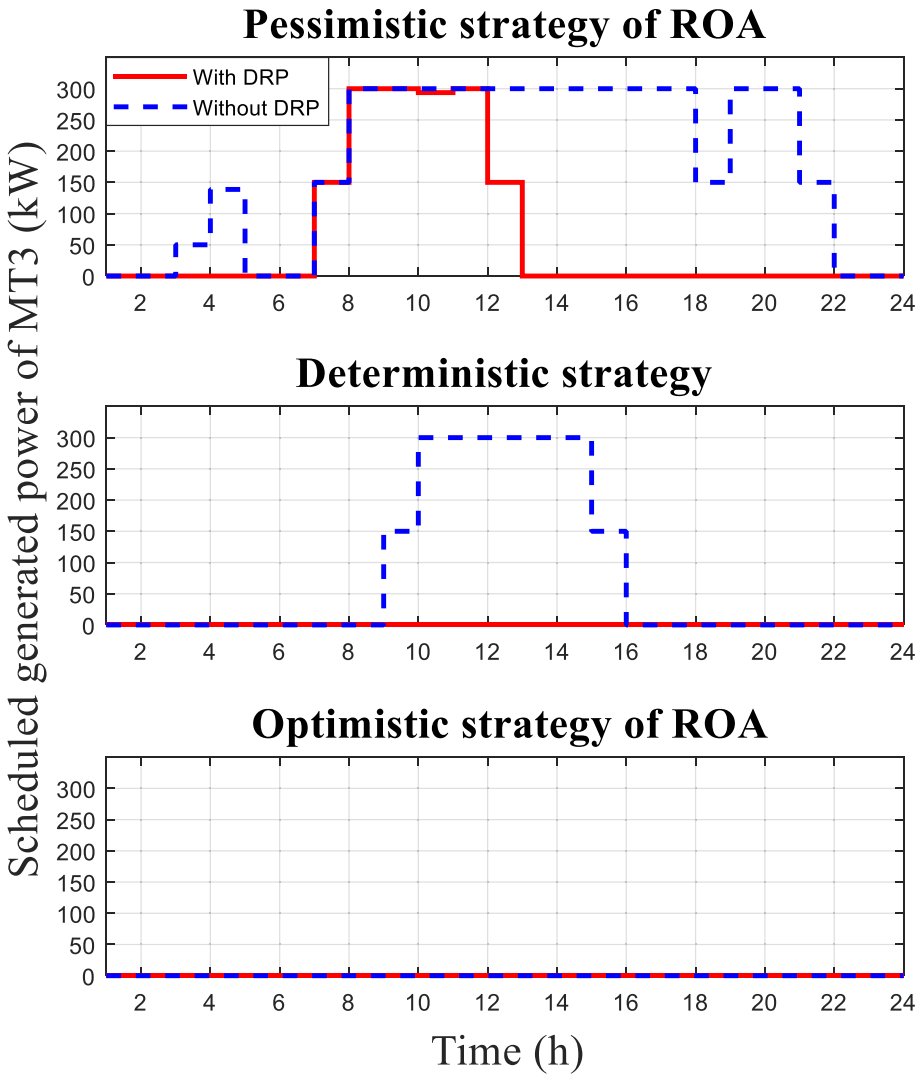

Fig. 8. Power generation of micro-turbine 3.

$$|P_{UG}^{t}| \le P_{UG}^{\max} \tag{42}$$

where $P_{UG}^{\max}$is the maximum interchanged energy between upstream-grid and IPL.

3. ROA-based risk constrained method

In order to study impact of different uncertain parameter on operation on the under study system, different method such as fuzzy modeling, stochastic programming, information gap decision theory, robust optimization, etc. have been developed [38,39]. The robust optimization approach (ROA) is a powerful risk-management tool which seeks to immune the system from harmful aspect of the uncertain parameter. Using the ROA, the system operator can determine the best and worst operation cases which are referred to optimistic and pessimistic strategies in this paper. The objective function of system (1) with the constraints (2)–(42) is an MIP formulation, which can be expressed as standard form as follow:

$$Minimize \quad \sum_{t=1}^{T} e_t x_t \tag{43}$$

Sb. to:

$$\sum_{t=1}^{T} a_{mt} x_t \le b_m, \quad m = 1, \ldots, M \tag{44}$$

$$x_t \ge 0, \quad t = 1, \ldots, T \tag{45}$$

$$x_t \in \{0, 1\} \quad for\ some\ t = 1, \ldots, T \tag{46}$$

In Eq. (43), $e_t$are assumed unknown but bounded parameters as objective function's coefficient. Therefore, the developed mixed-integer programming (MIP) model can be reformulate as RMIP optimization related to (43)–(48). In the above equations, to presents the deviation from the nominal coefficients (e_t), the new parameter $d_t$is introduced.

In addition, to control robustness level of the developed objective function, an integer parameter $\Gamma_0$is utilized. By assuming $\Gamma_0$equal to $|J_0|$, price the price deviations in the proposed objective

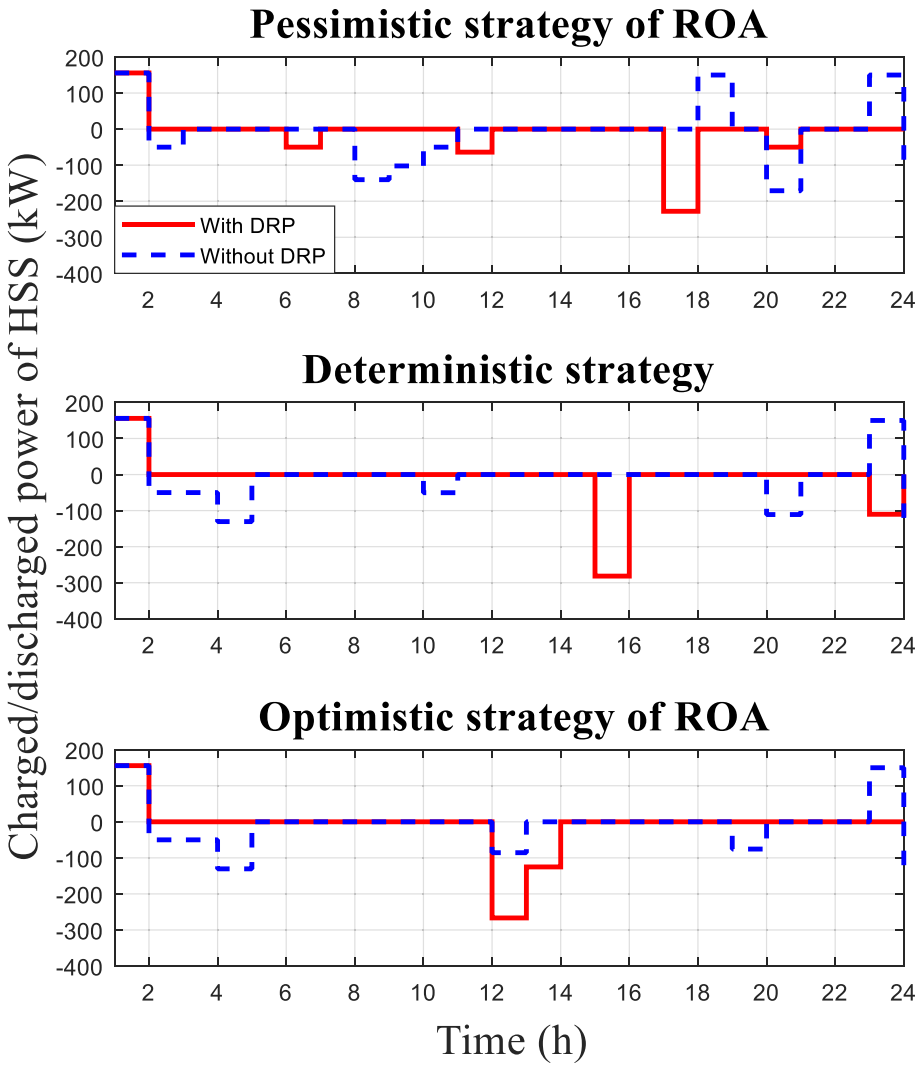

Fig. 9. Scheduled charged/discharged power of hydrogen storage system.

function can be considered. On the other hand, by setting $\Gamma_0$equal to zero, deviations of power price in the provided objective function will be ignored. Finally, RMIP optimization from of Eqs. (43)-(46) is reformulated based on linearizing technique and duality theorem as follow:

$$\underset{x_t,q_{ot},y_t,\ \forall t;z_0}{Minimize} \quad \sum_{t=1}^{T} e_t x_t + z_0\Gamma_0 + \sum_{t=1}^{T} q_{ot} \tag{47}$$

$$z_0 + q_{ot} \geq d_t y_t, \quad t \in J_0 \tag{48}$$

$$q_{ot} \geq 0, \quad t = 1,\ldots,T \tag{49}$$

$$y_t \geq 0, \quad t = 1,\ldots,T \tag{50}$$

$$z_0 \geq 0 \tag{51}$$

$$x_t \leq y_t, \quad t = 1,\ldots,T \tag{52}$$

In the above formulations, ancillary variable $y_t$is used to get the corresponding linear model. To consider the upper and lower bounds of the known parameters (e_t), variables $q_{ot}$and $z_0$are used as dual variables of Equations (43)-(46).

3.1. ROA based optimal scheduling of IPL

The RMIP problem for planning of IPL are considered as follow:

$$OBJ = \sum_{t=1}^{T}\left[\left(P_{UG}^{t}\times\pi_{UG}^{t} + \sum_{j=1}^{G}\left(C_{LDG}^{j,t} + SC_{LDG}^{j,t}\right) + \sum_{i=1}^{N}\left(-P_{Ch,EV}^{i,t} \times \pi_{Ch,EV}^{i} + P_{Dch,EV}^{i,t}\times\pi_{Dch,EV}^{i}\right)\right)\times\Delta t\right] + z_0\Gamma_0 + \sum_{t=1}^{T} q_t \tag{53}$$

$$z_0 + q_t \geq d_t \times y_t \quad t = 1,\ldots,T \tag{54}$$

$$q_t \geq 0 \quad t = 1,\ldots,T \tag{55}$$

$$q_t \geq 0 \quad t = 1,\ldots,T \tag{56}$$

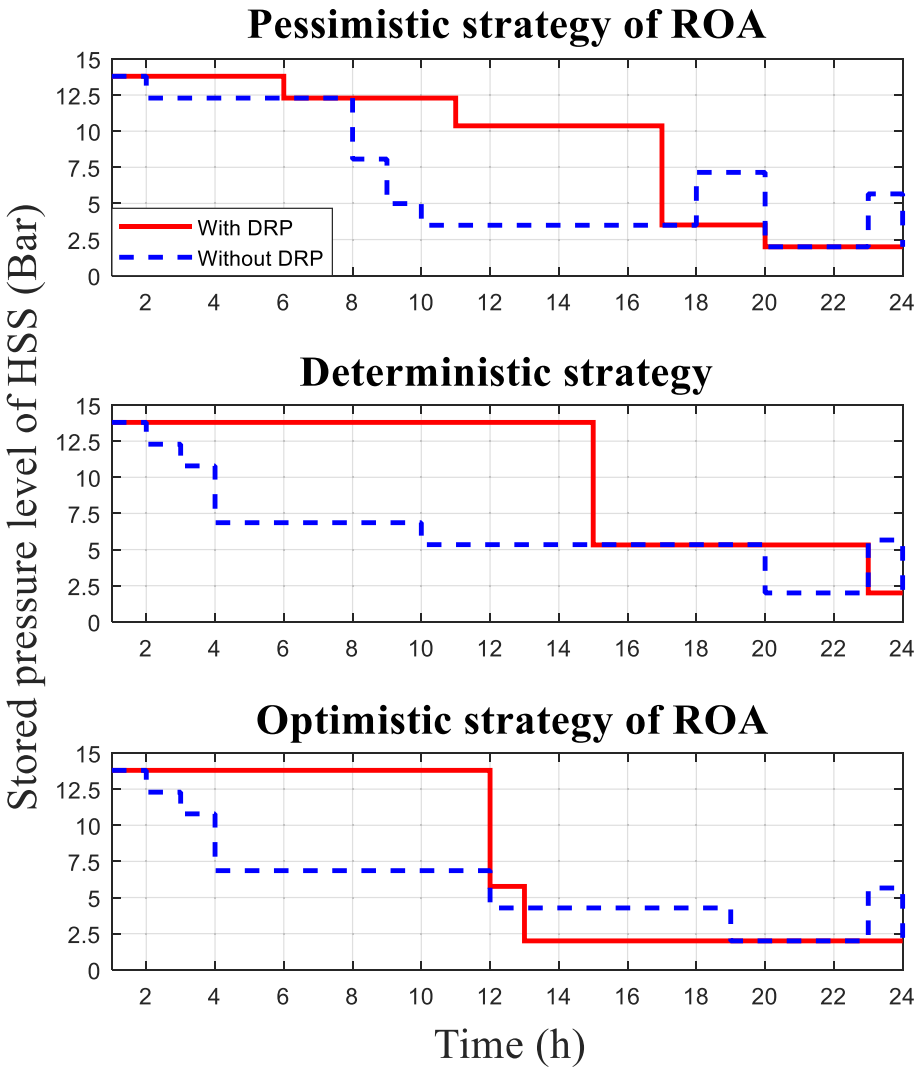

Fig. 10. Stored pressure level in the hydrogen storage system.

$$y_t \geq 0 \qquad t = 1, \ldots, T \tag{57}$$

$$z_0 \geq 0 \tag{58}$$

$$P^t_{grid} \leq y_t \qquad t = 1, \ldots, T \tag{59}$$

Constraints (2)–(42) (54)

$$\tilde{P}^t_{UG} < P^t_{UG}; \tilde{\pi}^t_{UG} > \pi^t_{UG} \tag{60}$$

Note that in order to get optimal hourly bidding curves for the IPL, the constraint (55) is added to the previous constraints [40]. The flowchart of the proposed algorithm is illustrated in Fig. 3. As it can be seen in Fig. 3, first it is required to set up market prices $\lambda_t = \lambda^{\min}_t (t = 1, \ldots, T)$. Also, the gamma value should be set as $\Gamma_0 = T$ which allows modeling of market prices deviations. In the second step, we should set up $d^k_t = G^k(\lambda^{\max}_t - \lambda^{\min}_t); (t = 1, \ldots, T)$. It should be noted that k is iteration counter and G^k takes rising values in $[0, 1]$ interval. In the third step, at each iteration k, the hourly scheduled power from the upstream grid is obtained by solving Eqs. (47)-(55). Steps 2 and 3 is recalculated for each iteration k. This process is implemented to calculate all G^k coefficients. In the final step, Step 4, the optimal bidding curves for the IPL is constructed in by using $\lambda^k_t = \lambda^{\min}_t + d^k_t (t = 1, \ldots, T)$.

4. Simulation results

In order to get optimal scheduling of the under study system and construct optimal bidding curves to submit to power market, the obtained results from ROA optimization are presented in three different strategies as optimistic, deterministic, and pessimistic strategies. As said before, the pessimist and optimistic strategies are developed to get worst and best cases of uncertainty parameter impact on the system operation while the problem is solved without considering uncertainty in the deterministic strategy to make a better comparison with two other strategies. To demonstrate the effect of DRP on the operation of the system, each strategy is solved in two cases as with and without DRP. Finally, the optimal hourly bidding curves for the IPL are provided which is the main goal of this study.

4.1. Robust operating cost

The total operation cost of the system is presented in Fig. 4. The

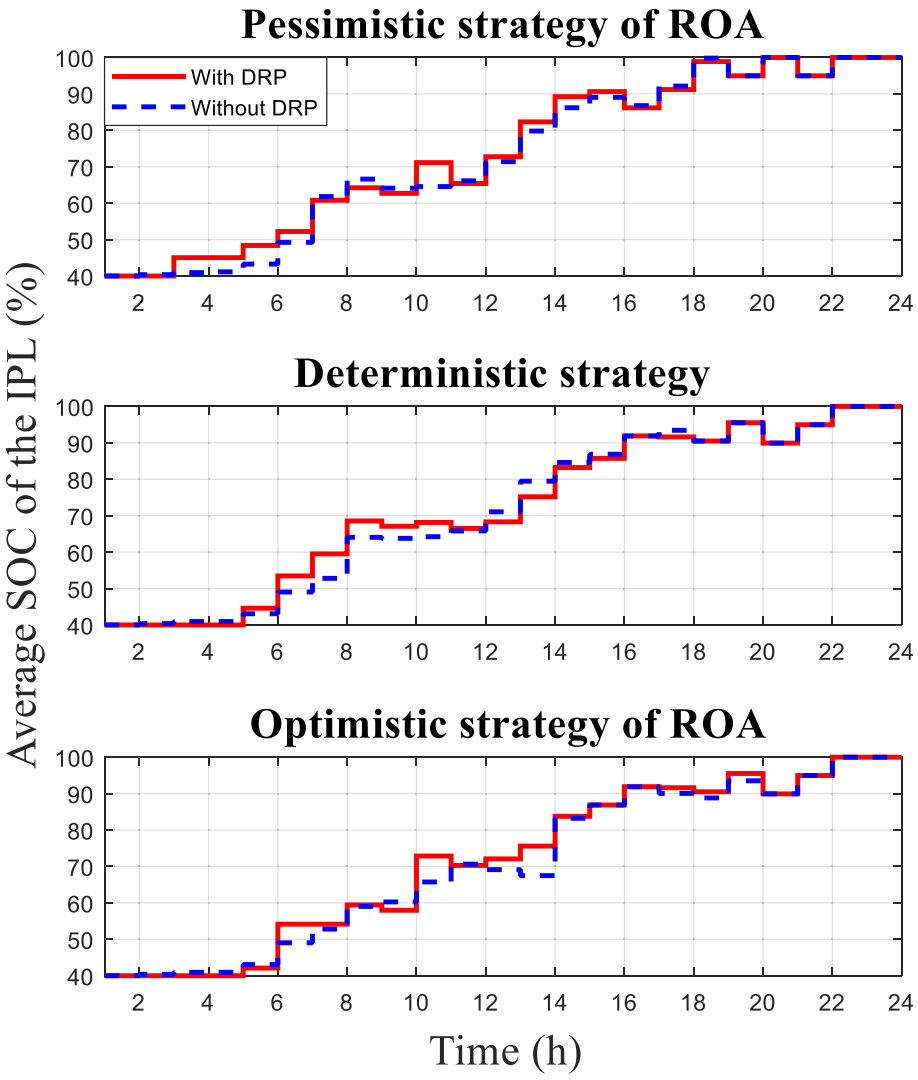

Fig. 11. SOC of the IPL

problem is solved in 11 iterations in which in the first iteration the obtained results are related to the optimistic iteration (considers best possible case for the uncertain parameter), results of sixth iteration is related to the determinist strategy, and finally in the last operation is presents the pessimistic strategy results which models worst possible case for the uncertainty of power price in the upstream-grid. In the optimistic strategy, robust system operating cost is obtained as $1017 and $995.1 for without and with DRP cases, indicating 2.15% reduction due to implementation of the DRP. In the deterministic case, which considers estimated power price without any uncertainty, total operating cost for without and with DRP cases are obtained as $1238 and $1,209, respectively. In this strategy, the DRP has reduced total operating cost about 2.34%. Finally, by considering worst case of uncertainty in the power price in the upstream-grid which models high prices, in the pessimistic strategy total operating cost is equal to $1360 and $1333 for without and with DRP cases, respectively. The obtained results are briefly presented in Table 1.

4.2. Load profile

Load profile of the system for all strategies considering with/without DRP cases are depicted in Fig. 5. The implemented TOU rate of DRP, as mentioned earlier, shifts load from high price periods to low price periods to reduce operating cost of the system. According to Fig. 5, in the deterministic case, the load is shifted from hours 5–9 to 10–15 and from 22 to 24 to 20–22. In addition, in the optimistic strategy the DRP transfers load from hours 20–24 to 10–14. As upstream-gird prices in pessimistic strategy is higher than two other strategies, load curve change due to DRP is considerable in comparison with deterministic or optimistic strategies. It is obvious that in all strategies, especially in pessimistic strategy, the load curve is flattened by implementing the DRP which will result in lower system operating cost. In the deterministic strategy, the maximum load change by the DRP is recorded at hour 7 in which the load is increased from 1795 kW to 2154 kW, indicating 20% increase in the base load. Also, in the optimistic strategy, the DRP has reduced load of the system from 1729 kW to 1383 kW at hour 13, which is equal to about 20% decrease in the base load. In addition, the load of system is increased from 1773 kW to 2127 kW at hour 11, presenting 19.9% increase in the base load profile of the system. In all strategies, load profile has not been changed at hour 18 in which the load amount is equal to 2160 kW.

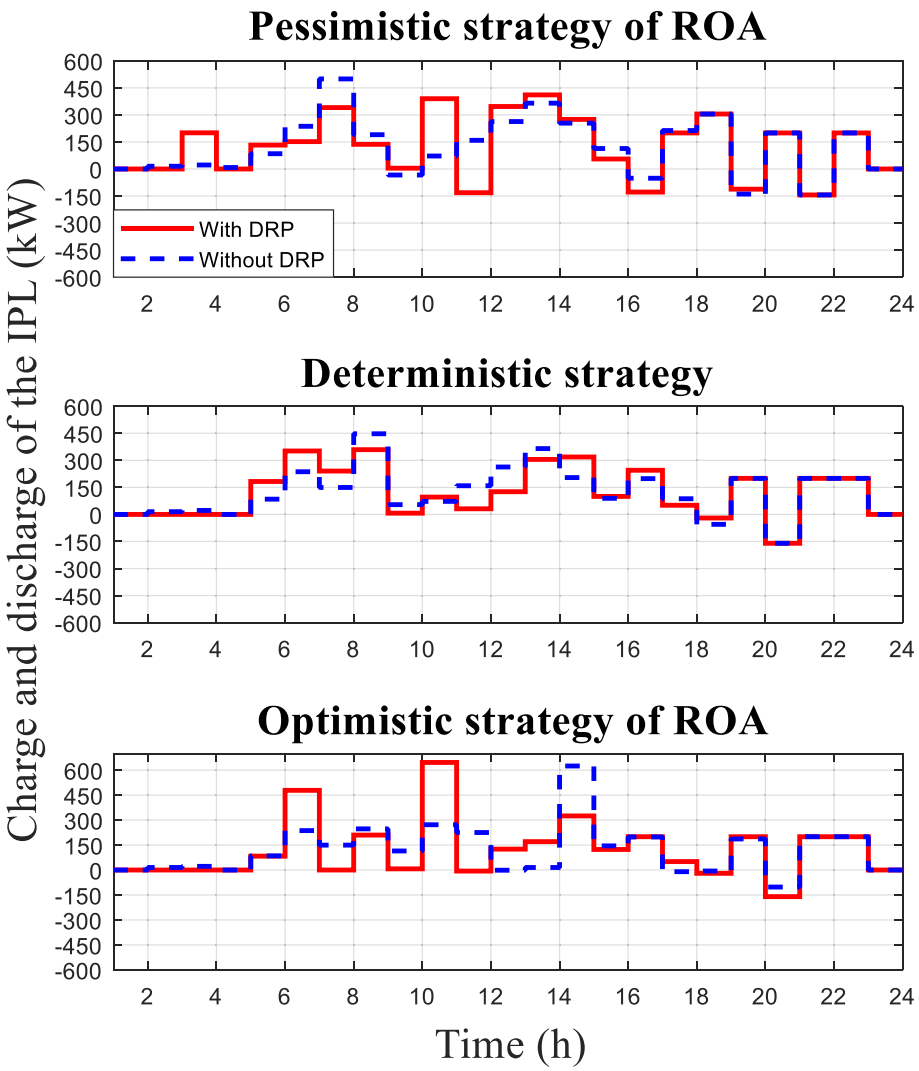

Fig. 12. Charging and discharging of the IPL.

4.3. Generated power by the MTs

Scheduled generated power by MTs 1–3 are depicted in Figs. 6–8, respectively. In Fig. 6, which shows the generated power of the MT1, the generated power by the MT1 is increased after implementing the DRP in pessimistic strategy. Note that as market prices are higher in the pessimistic strategy in comparison with other strategies, the system operator should rely more on its internal energy sources rather than purchasing power from the upstream-grid. It can be seen that there is a slight change in scheduled generated power by the MT1 in deterministic strategy after implementing DRP while the obtained results for with and without DRP cases are the same in the optimistic strategy. The MT1 power generation is equal to 700 kW during hours 6–21 in the pessimistic strategy. Also, the MT1 delivers the mentioned amount of power to the grid during hours 6–17 and 20, in the deterministic strategies. The same amount of power has been generated by the MT1 during hours 6–14, 16, and 19 in the optimistic strategy.

Power output of the MT2 is presented in Fig. 7. Generated power by the MT2 in pessimistic and deterministic cases is increased by implementing DRP program while in the optimistic strategy the power output of by the MT2 is not changed in without and with DR cases. In the deterministic strategy, the generated power by the MT2 is considerably increased after implementing the DRP to satisfy the required demand of the new load curve. Turning to Fig. 5, which depicts the load curve, the load demand in deterministic strategy is increased between hours 4–8. Therefore, the generated power by the MTs should be increased to satisfy the load. By considering the ramp-up and ramp-down rates of the MTs, it can be said that as MT1 is scheduled to generated power with its maximum capacity after hour 6, the considerable part of load increase after implementing DRP program is supplied by the MT2 in the deterministic strategy. In pessimistic strategy, by considering high prices in the upstream grid, the MTs are scheduled with their maximum capacity. Therefore, significant change is not seen in the generated power by the MT2 in the pessimistic strategy.

According to Fig. 7, The MT2 has generated power with its maximum available capacity during hours 9–17 and 19 in the pessimistic strategy, 10–13 in deterministic strategy, and 12–13 in the optimistic strategy which is equal to 400 kW. Considering the maximum load of the system in the with and without DRP cases in all strategies, which is equal to the 2160 kW, it can be said that during the mentioned hours the generated power by the MT2 is equal to 18.5% of the peak load of the system.

The scheduled power output of MT3 is shown in Fig. 8. Considering operating cost of the MT3 and significant increase of

generated power by the MT2 in deterministic strategy, power output of MT3 is zero after implementing the DRP program in the deterministic strategy. In the optimistic strategy, due to fair power prices in the upstream grid, the MT3 is not scheduled to generated power. The MT3 generates power with its maximum available capacity which is equal to 300 kW during hours 8–17, 19 and 20 in the without DRP case of pessimistic strategy, and during hours 8–12 in the with DRP case of the pessimistic strategy. In the deterministic case only in the without DRP case the MT3 delivers its maximum available power during hours 10–14.

4.4. Scheduling of the HSS

As an energy source to supply the load, charged/discharged power of the HSS is depicted in Fig. 9 in all strategies. Note the charged power is shown by the positive numbers while the negative numbers present the discharged power. The HSS in all strategies is charged during off peak periods and discharged in peak-periods. For example, in the pessimistic strategy, after implementing the DRP, the HSS is charged at hour 1–2 while it is mostly discharged at hour 18 which coincidence with the peak period at this case. Same thing can be said other strategies and cases. In the pessimistic strategy, the highest discharged power of the HSS is recorded at hour 20 in the without DRP case equal to 170.9 kW while the highest charged power to the HSS is equal to 155.8 kW recorded at hour 1. In the deterministic strategy, the maximum charged and discharged power is recorded as 155.8 and 281.5 kW at hours 1 and 15 in the without DRP case, respectively. The maximum charged and discharged power of the HSS are equal to 155.8 and 266.6 kW at hours 1 and 12 in the without DRP case in the optimistic strategy.

Stored pressure level in the HSS is depicted in Fig. 10. As there is no significant difference between the operation of the HSS in different strategies and cases, it can be said that obtained results in this case in similar to each other. It is obvious that the maximum amount of the stored pressure level is recorded in the with DRP case of the deterministic strategy which is equal to 13.8 Bar between hours 1 and 14.

4.5. Operation of the IPL

Fig. 11 depicts the state-of-charge (SOC) of the IPL. Considering operational constraints of the IPL including expected SOC of the parked EVs at the leaving, initial SOC level, and enter and EVs' leaving time, the SOC of the IPL is continuously increasing between hours 2–16 in all strategies and cases. It is obvious that in the all strategies and all cases, the SOC of the IPL reaches 100% of its capacity at hour 22 and stay fix until end of the time period.

The discharging/charging of the IPL is illustrated in Fig. 12 which is in observing of SOC of the IPL. According to Fig. 12, it is obvious that the IPL is charged the parked EVs during off-peak period and in some cases, to help the system operator, discharged the EVs considering their operational requirements.

According to the obtained results, the maximum amount of discharged power of the IPL is recorded at hour 20 in the deterministic strategy which is equal to 160 kW. On the other hand, the maximum charged power of the IPL is equal to 625 kW which is reported at hour 14 in the without DRP case of the optimistic strategy.

4.6. Optimal bidding curves

Providing the optimal bidding curve is the main goal of this study which is detailed in this sub-section. In restructured power systems, obtaining optimal bidding curves is required and necessary to take part in power market and purchase energy to satisfy required load demand by any electricity entity like retailers, large consumers, load serving entities, IPLs, etc. The importance of providing bidding (and offering) curves is increased by considering uncertainty of power price in market in which such curves help operator of the system to get required power to satisfy its load the best possible prices. In this paper, the hourly bidding curves are constructed which can be provided to the upstream grid in two different cases as without and with DR. It should be noted that the bidding curves should be steadily decreasing, as a common requirement in almost any power markets. Fig. 13 presents optimal bidding curve at hour 3 in with and without DRP cases. At this hour, it is obvious that due to fair power prices at the market, the system operator is eager to get 1000 kW from the market at any price which is predicted something between 0.013 and 0.021 $/kWh in both without and with DRP cases.

The optimal bidding curve at hour 15 is depicted in Fig. 14. It is obvious that total bid power in without DRP case in higher than with DR case due to implementing DRP has reduced load amount at this hour which was detailed in previous sub-sections. In the without DRP case, the bid power at hour 15 is equal to zero when market power price is between 0.081 and 0.093 $/kWh which means that the system operator finds these prices high and un-

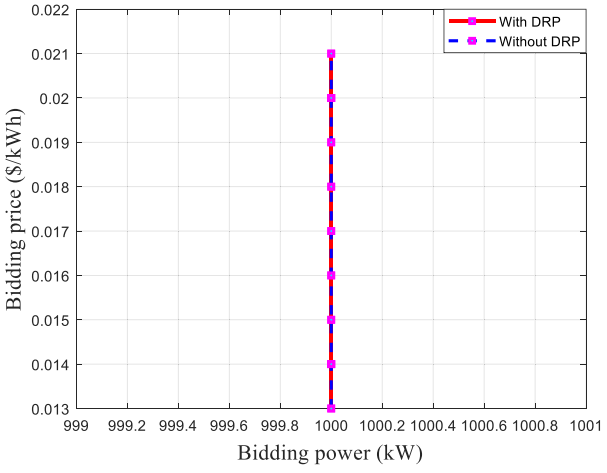

Fig. 13. Optimal bidding-curve of hour 3.

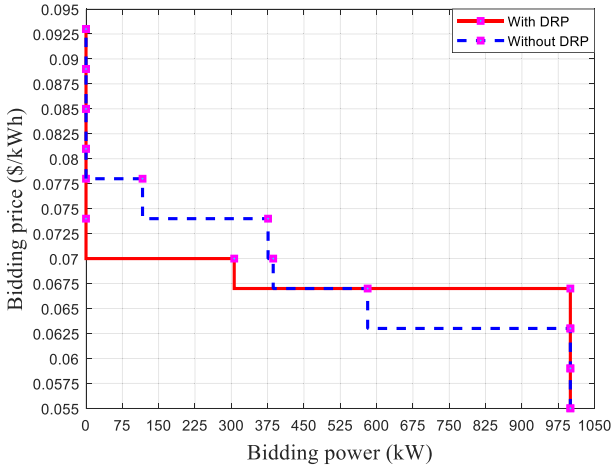

Fig. 14. Optimal bidding-curve of hour 15.

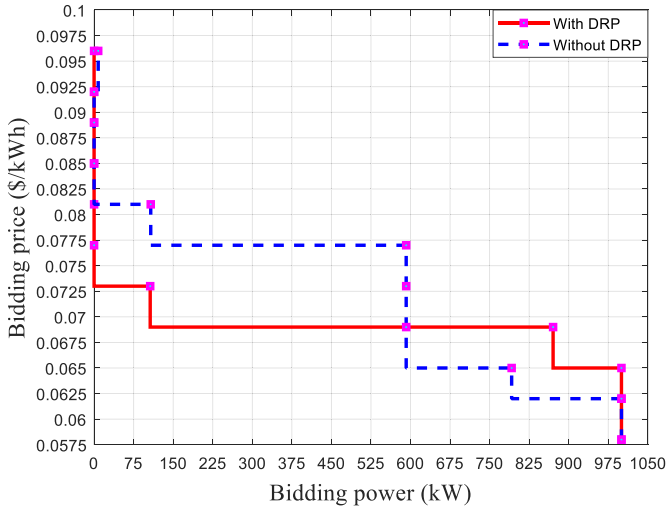

Fig. 15. Optimal bidding-curve of hour 21.

economical to get power from the upstream-grid. On the other hand, by decreasing market price, bid power of the system operator is increased in which when market price reaches to 0.055 $/kWh, the highest bid power is reported equal to 100 kW. By implementing DRP at hour 15, the system operator does not take part in the power market when the price is upper than 0.074 $/kWh. A, the maximum amount of bid power is provided when power price is lower or equal to 0.067 $/kWh.

Finally, the optimal bidding curve at hour 21 is depicted in Fig. 15. As it can be seen, when market price is higher than 0.085 and 0.077 $/kWh the bid power is equal to zero for without and with DRP cases, respectively. By reducing market price, the bid power is increased in both cases in which when power price is less than 0.062 and 0.065 $/kWh, the bid power reaches its highest amount in without and with DRP cases which is equal to 1000 kW. It should be noted that according to considered constraint for transfer power from the upstream grid, only 1000 kW can be purchased from the power market at each hour.

5. Discussion

The problem of optimal participation of IPLs in the power market is studied by developing a novel robust strategy to provide optimal bidding curves. In this paper the problem is modeled as RMIP which is solved using the GAMS software. The total simulation time for this study is equal to 26.886 s including 42 blocks of equations and, 23 block of variables, and 600 discrete variables for each iteration. According to the obtained results, the total operating cost of the system due to the power price uncertainty can vary from $1017 to $1360 in without DRP case. By implementing the DRP model, operating cost of the system can change from $995.1 to $1333. These numbers means that by applying the DRP, maximum 2.15 and minimum 1.98% reduction of system operating cost can be attained because of the DRP. Also, planning of each component of the system is surveyed in the previous sections. In addition, the optimal bidding curves to procure energy form the upstream grid is extracted for each hour which can help the system operator to purchase power from the upstream grid with a reasonable price. These curves are provided to the day-ahead power market.

6. Conclusion

By increasing concerns of greenhouse gases emission, finding new ways to reduce emission is inevitable. In order to reduce generated emission by the transportation which constitutes considerable portion of emission, attentions to EVs are increased day by day. Integration of EVs into power system has different challenges due to theirs high uncertainty level. Therefore, in this paper the concept of IPL is used to solve various challenge of EVs integration to the power system. On the other hand, in order to optimally schedule the system and participate in the power market, a novel ROA based method is proposed to develop optimal bidding curve for IPL. The main purpose of this paper was to provide optimal bidding curves to submit to the day-ahead power markets. Using the provided optimal bidding curve, the system operator can get required power to satisfy demand of parked EVs in the IPL with the best and economical price in the presence of uncertain power prices uncertainty in the power market. Simulations are executed on a system including wind-turbine, micro-turbines, HSS, upstream grid, and IPL. Optimal planning of each component of the system is carried out in three different strategies as optimistic, deterministic, and pessimistic to consider all possible cases raised by power price uncertainty. The problem has been formulated as RMIP which is solved using the GAMS optimization software under CPLEX solver. According to the obtained results by applying DRP, total operating cost of the system has reduced because of flattening the load curve. Comparing obtained results with the deterministic case, the total operating cost of the system is decreased from $1029 to $995 about 17.85% decrease while in pessimistic strategy, it is increased from $1209 to $1333 indicating about 9.85% increase. Finally, system's different parts planning and optimal bidding curve of the IPL for different hours are detailed in the context.

Declaration of competing interest

The authors declare that they have no known competing financial interests or personal relationships that could have appeared to influence the work reported in this paper.

CRediT authorship contribution statement

Jianwei Guo: Data curation, Formal analysis, Funding acquisition, Investigation, Methodology, Project administration, Resources, Software, Supervision, Validation, Visualization, Writing - original draft, Writing - review & editing. **Yongbo Lv:** Data curation, Formal analysis, Investigation, Methodology, Resources, Software, Supervision, Validation, Visualization, Writing - original draft, Writing - review & editing. **Han Zhang:** Data curation, Formal analysis, Investigation, Methodology, Resources, Software, Supervision, Validation, Visualization, Writing - original draft, Writing - review & editing. **Sayyad Nojavan:** Conceptualization, Data curation, Formal analysis, Investigation, Methodology, Software, Validation, Visualization, Writing - review & editing. **Kittisak Jermsittiparsert:** Project administration, Resources, Supervision, Validation, Visualization, Writing - review & editing.

Acknowledgement

This research is supported by National Natural Science Foundation of China (No. 61872036) and National key technologies Research & Development program (No. 2017YFC0804900).

References

[1] Ozturk M, Dincer I. Comparative environmental impact assessment of various fuels and solar heat for a combined cycle. Int J Hydrogen Energy 2019;44:5043–53. https://doi.org/10.1016/J.IJHYDENE.2019.01.003.
[2] Shamsi H, Haghi E, Raahemifar K, Fowler M. Five-year technology selection optimization to achieve specific CO2 emission reduction targets. Int J

Hydrogen Energy 2019;44:3966–84. https://doi.org/10.1016/J.IJHYDENE.2018.12.104.
[3] Xiong H, Liu H, Zhang R, Yu L, Zong Z, Zhang M, et al. An energy matching method for battery electric vehicle and hydrogen fuel cell vehicle based on source energy consumption rate. Int J Hydrogen Energy 2019;44:29733–42. https://doi.org/10.1016/J.IJHYDENE.2019.02.169.
[4] Tanç B, Arat HT, Baltacıoğlu E, Aydın K. Overview of the next quarter century vision of hydrogen fuel cell electric vehicles. Int J Hydrogen Energy 2019;44:10120–8. https://doi.org/10.1016/J.IJHYDENE.2018.10.112.
[5] Mohiti M, Monsef H, Lesani H. A decentralized robust model for coordinated operation of smart distribution network and electric vehicle aggregators. Int J Electr Power Energy Syst 2019;104:853–67. https://doi.org/10.1016/J.IJEPES.2018.07.054.
[6] Anastasiadis AG, Konstantinopoulos S, Kondylis GP, Vokas GA. Electric vehicle charging in stochastic smart microgrid operation with fuel cell and RES units. Int J Hydrogen Energy 2017;42:8242–54. https://doi.org/10.1016/J.IJHYDENE.2017.01.208.
[7] Marzoghi AF, Bahramara S, Adabi F, Nojavan S. Optimal scheduling of intelligent parking lot using interval optimization method in the presence of the electrolyser and fuel cell as hydrogen storage system. Int J Hydrogen Energy 2019;44:24997–5009. https://doi.org/10.1016/J.IJHYDENE.2019.07.226.
[8] Rezaee S, Farjah E, Khorramdel B. Probabilistic analysis of plug-in electric vehicles impact on electrical grid through homes and parking lots. IEEE Trans Sustain Energy 2013;4:1024–33. https://doi.org/10.1109/TSTE.2013.2264498.
[9] Zhang L, Li Y. A game-theoretic approach to optimal scheduling of parking-lot electric vehicle charging. IEEE Trans Veh Technol 2016;65:4068–78. https://doi.org/10.1109/TVT.2015.2487515.
[10] Zhang L, Li Y. Optimal management for parking-lot electric vehicle charging by two-stage approximate dynamic programming. IEEE Trans Smart Grid 2017;8:1722–30. https://doi.org/10.1109/TSG.2015.2505298.
[11] Kuran MS, Carneiro Viana A, Iannone L, Kofman D, Mermoud G, Vasseur JP. A smart parking lot management system for scheduling the recharging of electric vehicles. IEEE Trans Smart Grid 2015;6:2942–53. https://doi.org/10.1109/TSG.2015.2403287.
[12] Shafie-khah M, Heydarian-Forushani E, Osorio GJ, Gil FAS, Aghaei J, Barani M, et al. Optimal behavior of electric vehicle parking lots as demand response aggregation agents. IEEE Trans Smart Grid 2016;7:2654–65. https://doi.org/10.1109/TSG.2015.2496796.
[13] Mirzaei MJ, Kazemi A, Homaee O. A probabilistic approach to determine optimal capacity and location of electric vehicles parking lots in distribution networks. IEEE Trans Ind Informatics 2016;12:1963–72. https://doi.org/10.1109/TII.2015.2482919.
[14] Akhavan-Rezai E, Shaaban MF, El-Saadany EF, Karray F. Online intelligent demand management of plug-in electric vehicles in future smart parking lots. IEEE Syst J 2016;10:483–94. https://doi.org/10.1109/JSYST.2014.2349357.
[15] Ruiz-Rodriguez FJ, Hernández JC, Jurado F. Voltage behaviour in radial distribution systems under the uncertainties of photovoltaic systems and electric vehicle charging loads. Int Trans Electr Energy Syst 2018;28:e2490. https://doi.org/10.1002/etep.2490.
[16] Gomez-Gonzalez M, Hernandez JC, Vera D, Jurado F. Optimal sizing and power schedule in PV household-prosumers for improving PV self-consumption and providing frequency containment reserve. Energy 2020;191:116554. https://doi.org/10.1016/j.energy.2019.116554.
[17] Hernández JC, Ruiz-Rodriguez FJ, Jurado F. Modelling and assessment of the combined technical impact of electric vehicles and photovoltaic generation in radial distribution systems. Energy 2017;141:316–32. https://doi.org/10.1016/j.energy.2017.09.025.
[18] Chukwu UC, Mahajan SM. V2G parking lot with PV rooftop for capacity enhancement of a distribution system. IEEE Trans Sustain Energy 2014;5:119–27. https://doi.org/10.1109/TSTE.2013.2274601.
[19] Yazdani-Damavandi M, Moghaddam MP, Haghifam M-R, Shafie-khah M, Catalao JPS. Modeling operational behavior of plug-in electric vehicles' parking lot in multienergy systems. IEEE Trans Smart Grid 2016;7:124–35. https://doi.org/10.1109/TSG.2015.2404892.
[20] Jannati M, Hosseinian SH, Vahidi B, Li G. A significant reduction in the costs of battery energy storage systems by use of smart parking lots in the power fluctuation smoothing process of the wind farms. Renew Energy 2016;87:1–14. https://doi.org/10.1016/J.RENENE.2015.09.054.
[21] Bonges HA, Lusk AC. Addressing electric vehicle (EV) sales and range anxiety through parking layout, policy and regulation. Transport Res Part A Policy Pract 2016;83:63–73. https://doi.org/10.1016/J.TRA.2015.09.011.
[22] Honarmand M, Zakariazadeh A, Jadid S. Integrated scheduling of renewable generation and electric vehicles parking lot in a smart microgrid. Energy Convers Manag 2014;86:745–55. https://doi.org/10.1016/J.ENCONMAN.2014.06.044.
[23] Honarmand M, Zakariazadeh A, Jadid S. Self-scheduling of electric vehicles in an intelligent parking lot using stochastic optimization. J Franklin Inst 2015;352:449–67. https://doi.org/10.1016/J.JFRANKLIN.2014.01.019.
[24] Iversen EB, Morales JM, Madsen H. Optimal charging of an electric vehicle using a Markov decision process. Appl Energy 2014;123:1–12. https://doi.org/10.1016/J.APENERGY.2014.02.003.
[25] Zakariazadeh A, Jadid S, Siano P. Multi-objective scheduling of electric vehicles in smart distribution system. Energy Convers Manag 2014;79:43–53. https://doi.org/10.1016/J.ENCONMAN.2013.11.042.
[26] Fazelpour F, Vafaeipour M, Rahbari O, Rosen MA. Intelligent optimization to integrate a plug-in hybrid electric vehicle smart parking lot with renewable energy resources and enhance grid characteristics. Energy Convers Manag 2014;77:250–61. https://doi.org/10.1016/J.ENCONMAN.2013.09.006.
[27] Moradijoz M, Parsa Moghaddam M, Haghifam MR, Alishahi E. A multi-objective optimization problem for allocating parking lots in a distribution network. Int J Electr Power Energy Syst 2013;46:115–22. https://doi.org/10.1016/J.IJEPES.2012.10.041.
[28] El-Zonkoly A, dos Santos Coelho L. Optimal allocation, sizing of PHEV parking lots in distribution system. Int J Electr Power Energy Syst 2015;67:472–7. https://doi.org/10.1016/J.IJEPES.2014.12.026.
[29] Song J, Krishnamurthy V, Kwasinski A, Molina R. Analysis of the energy storage operation of electrical vehicles with a photovoltaic roof using a Markov chain model. In: Ieee veh. Power propuls. Conf. IEEE; 2012. p. 820–5. 2012.
[30] Yu D, Xu X, Dong M, Nojavan S, Jermsittiparsert K, Abdollahi A, et al. Modeling and prioritizing dynamic demand response programs in the electricity markets. Sustain Cities Soc 2020;53:101921. https://doi.org/10.1016/J.SCS.2019.101921.
[31] Ghalelou AN, Fakhri AP, Nojavan S, Majidi M, Hatami H. A stochastic self-scheduling program for compressed air energy storage (CAES) of renewable energy sources (RESs) based on a demand response mechanism. Energy Convers Manag 2016;120:388–96. https://doi.org/10.1016/J.ENCONMAN.2016.04.082.
[32] Aalami HA, Pashaei-Didani H, Nojavan S. Deriving nonlinear models for incentive-based demand response programs. Int J Electr Power Energy Syst 2019;106. https://doi.org/10.1016/j.ijepes.2018.10.003.
[33] Borowy BS, Salameh ZM. Optimum photovoltaic array size for a hybrid wind/PV system. IEEE Trans Energy Convers 1994;9:482–8. https://doi.org/10.1109/60.326466.
[34] Valverde L, Rosa F, Bordons C, Guerra J. Energy management strategies in hydrogen smart-grids: a laboratory experience. Int J Hydrogen Energy 2016;41:13715–25. https://doi.org/10.1016/J.IJHYDENE.2016.05.279.
[35] Cau G, Cocco D, Petrollese M, Knudsen Kær S, Milan C. Energy management strategy based on short-term generation scheduling for a renewable microgrid using a hydrogen storage system. Energy Convers Manag 2014;87:820–31. https://doi.org/10.1016/J.ENCONMAN.2014.07.078.
[36] Pashaei-Didani H, Nojavan S, Nourollahi R, Zare K. Optimal economic-emission performance of fuel cell/CHP/storage based microgrid. Int J Hydrogen Energy 2019;44:6896–908. https://doi.org/10.1016/J.IJHYDENE.2019.01.201.
[37] Honarmand M, Zakariazadeh A, Jadid S. Optimal scheduling of electric vehicles in an intelligent parking lot considering vehicle-to-grid concept and battery condition. Energy 2014;65:572–9. https://doi.org/10.1016/J.ENERGY.2013.11.045.
[38] Chen Z, Wu L, Fu Y. Real-time price-based demand response management for residential appliances via stochastic optimization and robust optimization. IEEE Trans Smart Grid 2012;3:1822–31. https://doi.org/10.1109/TSG.2012.2212729.
[39] Nojavan S, Ghesmati H, Zare K. Robust optimal offering strategy of large consumer using IGDT considering demand response programs. Elec Power Syst Res 2016;130:46–58. https://doi.org/10.1016/J.EPSR.2015.08.017.
[40] Nojavan S, Pashaei-Didani H, Saberi K, Zare K. Risk assessment in a central concentrating solar power plant. Sol Energy 2019;180. https://doi.org/10.1016/j.solener.2019.01.024.